31st Annual International Conference of the IEEE EMBS
Minneapolis, Minnesota, USA, September 2-6, 2009

A Comparison of Data-Independent Microwave Beamforming Algorithms for the Early Detection of Breast Cancer

Dallan Byrne, Martin O'Halloran, Edward Jones and Martin Glavin

Abstract— **Ultrawideband (UWB) radar is one of the most promising alternatives to X-ray mammography as an imaging modality for the early detection of breast cancer. Several beamforming algorithms have been developed which exploit the dielectric contrast between normal and cancerous tissue at microwave frequencies in order to detect tumors. Dielectric heterogeneity within the breast greatly effects the ability of a beamformer to detect very small tumors, therefore the design of an effective beamformer for this application represents a significant challenge. This paper analyzes and compares 3 data-independent beamforming algorithms, testing each system on an anatomically correct, MRI derived breast model which incorporates recently-published data on dielectric properties.**

I. Introduction

Breast cancer is one of the most common cancers to affect women. Each year in the U.S alone, approximately 182,000 cases are diagnosed [1]. Early detection and intervention is one of the most significant factors in improving the survival rates and quality of life experienced by breast cancer sufferers [2]. X-ray mammography is the current *defacto* screening method for detecting non-palpable, early stage breast cancer. The inherent limitations of X-ray mammography are well documented [2].

One of the most promising emerging breast imaging modalities is microwave imaging. Ultrawideband (UWB) Radar imaging, as proposed by Hagness *et al.* [3], uses reflected UWB signals to determine the location of microwave scatterers within the breast. Data-independent beamforming algorithms have been developed to synthetically focus the returns from a particular point within the breast [4], [5], and to compensate for frequency-dependent attenuation and phase effects [6], [7], [8].

Dielectric examinations of breast tissue originally carried out by Chaudhary, Joines and Jossinet *et al.* [9], [10], [11] indicated substantial dielectric contrasts between normal and malignant breast tissues at frequencies up to 1MHz. The recently established dielectric contrast between adipose and fibroglandular tissue at microwave frequencies presents a more challenging imaging scenario where clutter is much more significant. This prompts the development of more robust imaging algorithms to mitigate the effects of increased clutter and to accurately determine the presence and location of any cancerous tissue within the breast. This paper presents an overview of 3 data-independent beamforming algorithms applied to near field breast imaging scenarios with identical dielectric and geometrical properties. In this paper data adaptive beamformers are not investigated as there may not be enough statistically independent observations to estimate a data covariance matrix [12], causing difficulty in a realistic breast imaging scenario. The rest of this paper is organized as follows: Section II and Section III describe the monostatic and multistatic Delay-and-Sum beamforming method, respectively. The Delay-Multiply-and-Sum beamformer is described in Section IV, followed by an examination of the MIST system in Section V and Section VI. Section VII describes the MRI derived breast model and simulation environment, along with a description of the compared beamformer results. Finally, concluding remarks are summarized in Section VIII.

The authors wish to thank IRCSET(Irish Research Council for Science, Engineering and Technology), Hewlett Packard (HP) and Science Foundation Ireland (SFI) for supporting this research.

Dallan Byrne, Martin O Halloran, Edward Jones and Martin Glavin are with Bioelectronics Research Cluster, NCBES, National University of Ireland, Galway, Ireland. email: dallan.byrne@nuigalway.ie

II. Monostatic Delay-and-Sum Beamforming

The monostatic Delay-and-Sum (DAS) beamformer is based on the Confocal Microwave Imaging (CMI) approach [3]. In the monostatic case, each antenna in turn illuminates the breast, and the reflected energy is recorded only at the transmitting antenna. The DAS beamformer involves time-shifting and summing the backscattered signals from the breast to create a synthetic focus. If a tumor exists at a specific focal point, then the returns from the tumor will add coherently. Returns from clutter due to natural heterogeneous tissue will add incoherently, and therefore will be suppressed. The energy at this synthetic focus is measured and stored, and an energy profile of the breast is created by varying the position of the synthetic focus within the breast. Consider M monostatic antennas, and let S_n denote the n^{th} backscattered signal, then the energy associated with point $\mathbf{r}$ within the breast is defined as:

$$I(\mathbf{r}) = \left[\sum_{n=1}^{M} S_n \left(\tau_n \left(r \right) \right) \right]^2 \tag{1}$$

where $\tau_n(\mathbf{r})$ is the round-trip time delay.

In order to compensate for attenuation and radial spreading of the UWB pulse within the breast, weighted DAS beamformers were developed by both Li *et al.* [13] and Fear *et al.* [5].

III. Multistatic Delay-and-Sum Beamforming

A multistatic DAS beamformer was developed by Nilavalan *et al.* [14]. In a multistatic system, the breast is illuminated by each antenna sequentially and the backscatter energy is recorded at every element in the antenna array. All received signals propagate out from the synthetic focal

point in different paths to acquire more information about the tumor. The energy at the focal point $\mathbf{r}$ for received signals $y_n(t)$ is described as:

$$I(\mathbf{r}) = \int_0^{\tau} \left(\sum_{n=1}^{M(M-1)/2} w_n y_n \left(t - T_n\right) \right)^2 dt \qquad (2)$$

where τ describes the transmit pulse width, T_n is the propagation time from the transmitting antenna to the receiving antenna and w_n is a compensation factor.

IV. Multistatic Delay-Multiply-and-Sum Beamforming

Another variant of the simple delay and sum beamformer is the Delay-Multiply-and-Sum (DMAS) beamformer developed by Lim *et al.* [15]. This algorithm involves signals being time-shifted, multiplied in pairs and their products summed to form the synthetic focal point. Energy at the synthetic focal point $\mathbf{r}$ is described by

$$I(\mathbf{r}) = \int_0^{W_l} S(n)\, dt \qquad (3)$$

Where W_l is the window length and $S(n)$ represents the backscatter signal after pair multiplication, summation and squaring. The paired multiplication increases the complexity and therefore the computation time significantly, compared to DAS. The DMAS approach was tested with a homogenous breast model with dielectric data similar to those used by Fear *et al.* [5].

V. Monostatic MIST Beamforming

Finally, Microwave Imaging via Space-Time (MIST) Beamforming was developed by Bond *et al.* to more effectively compensate for frequency-dependent propagation effects [6], [7]. The signals are firstly coarsely time-aligned, then passed through a bank of FIR filters which compensates for the propagation effects. Therefore, assuming the time-alignment step has been completed, the filter coefficients must satisfy the following equation:

$$\sum_{i=0}^{N} \tilde{S_{ii}}(\mathbf{r_0}, \omega) \mathbf{w_i^T} \mathbf{d}(\omega) \approx e^{-j\omega T_s (L-1)/2} \qquad (4)$$

where $S_{ii}(\mathbf{r_0}, \omega)$ is a model of the channel which affects the input signal as it propagates to and from the i^{th} transmitting antenna to the target over a time $T_{rt(i)}$, and is defined as follows:

$$S_{ii}(\mathbf{r_0}, \omega) = \left[\frac{1}{\sqrt{T_{rt(i)}}} e^{-\alpha(\omega) T_{rt(i)}} e^{-j\beta(\omega) T_{rt(i)}} \right] \qquad (5)$$

Where $\alpha(\omega)$ is the frequency-dependent attenuation factor and $\beta(\omega)$ is the frequency-dependant phase constant.

VI. Multistatic MIST Beamforming

Bond's *et al.* [6] monostatic MIST beamformer was further developed for application to multistatic signals by O'Halloran *et al.* [16]. Once the signals are time aligned, a redesigned FIR filter is used to equalize path length dispersion and attenuation for a multistatic imaging scenario. For a given focal point $\mathbf{r_0}$ within the breast, the effects of path-dependent attenuation and dispersion need to be mitigated. Therefore, assuming the time-alignment step has been completed, the filter coefficients must satisfy the following equation:

$$\sum_{i=0}^{N} \tilde{S_{ij}}(\mathbf{r_0}, \omega) \mathbf{w_{ij}^T} \mathbf{d}(\omega) \approx e^{-j\omega T_s (L-1)/2} \qquad (6)$$

where $S_{ij}(\mathbf{r_0}, \omega)$ is a model of the channel which affects the input signal as it propagates from the i^{th} transmitting antenna to the target, and back to the j^{th} receiving antenna over a time $T_{rt(i,j)}$, and is defined as follows:

$$S_{ij}(\mathbf{r_0}, \omega) = \left[\frac{1}{\sqrt{T_{rt(i,j)}}} e^{-\alpha(\omega) T_{rt(i,j)}} e^{-j\beta(\omega) T_{rt(i,j)}} \right] \qquad (7)$$

TABLE I
Debye parameters for the FDTD model

Tissue	ϵ_r	χ_1	σ	t_0
Skin	15.63	8.2	0.82	12.6
Tumor	7	47	0.15	7
Adipose (Low)	3.10	1.70	0.036	14
Fibroglandular (Low)	11	38	0.738	12
Adipose (Medium)	3.20	1.65	0.035	16
Fibroglandular (Medium)	11.2	38	0.738	12
Adipose (High)	4.75	2.95	0.083	15.5
Fibroglandular (High)	15.2	39	0.738	12.75

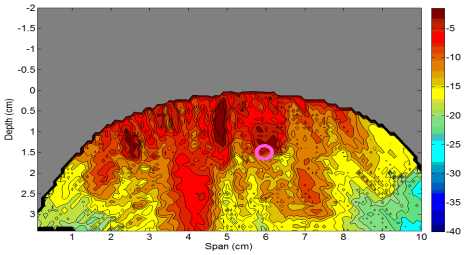

(a) Monostatic DAS

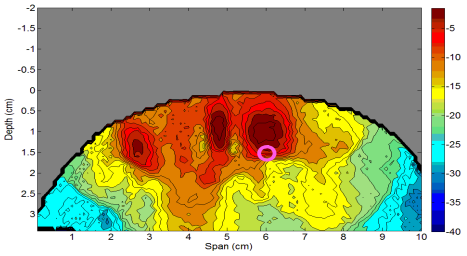

(b) Multistatic DAS

Fig. 1. DAS Beamformed Image with a malignant lesion a depth of 1.5 cm and span of 6 cm

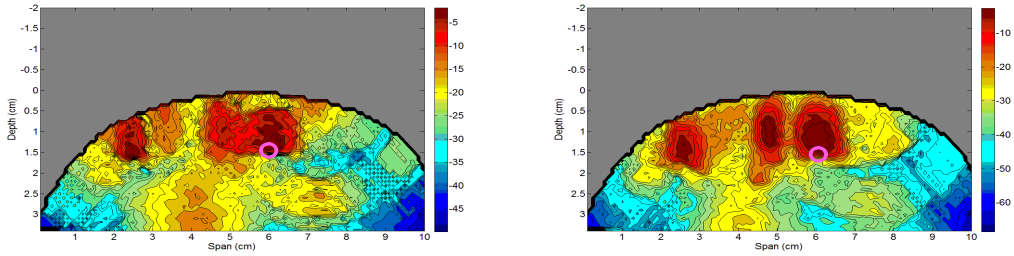

(a) Monostatic DMAS (b) Multistatic DMAS

Fig. 2. DMAS Beamformed Image with a malignant lesion a depth of 1.5 cm and span of 6 cm

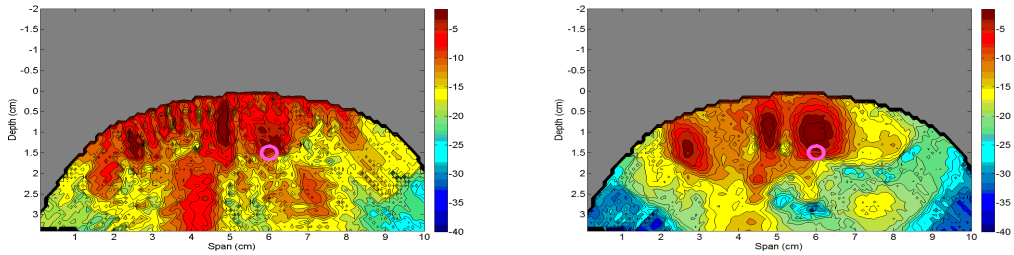

(a) Monostatic MIST (b) Multistatic MIST

Fig. 3. MIST Beamformed Image with a malignant lesion a depth of 1.5 cm and span of 6 cm

TABLE II
S/C RESULTS FOR 2 TUMOR POSITIONS

Beamformer	Location (Depth, Span) (cm)	S/C Multi (dB)	S/C Mono (dB)
DAS	(1.5, 6.0)	7.59	3.8
DAS	(1.5, 4.0)	9.57	2.73
MIST	(1.5, 6.0)	8.81	4.87
MIST	(1.5, 4.0)	12.37	4.72
DMAS	(1.5, 6.0)	14.27	10.86
DMAS	(1.5, 4.0)	25.05	9.3

VII. EVALUATION AND RESULTS

All backscatter data is obtained using a 2D finite-difference time-domain FDTD model of the breast [17], [18]. The model is that of a naturally flattened breast from a patient lying in the supine position. The adipose/fibroglandular tissue distribution is derived form an anatomically correct breast phantom, similar to the 2D model developed by Li *et al.* [13]. A tumor of 10mm in diameter is used in the FDTD models. A conformal equidistant array consisting of 14 antenna elements modeled as electric current sources are located on the surface of the naturally flattened breast, represented by dots in Figure 4, where fibroglandular regions appear as white and the adipose tissue as black. The model includes a 2mm layer of skin. The dispersive properties of breast tissue are incorporated into the FDTD model using a single-pole Debye model [19] of the following form:

$$\epsilon_r^*(\omega) = \epsilon_r + \frac{\sigma}{j\omega\epsilon_0} + \frac{\chi_1}{1 + j\omega t_0} \tag{8}$$

The dielectric properties of adipose and fibroglandular tissue used in the FDTD model are based on a recent study from Lazebnik *et al.* [20], [21]. A specific location within the FDTD model is defined as follows $(depth, span)$. For test purposes, a malignant tumor is located at (1.5 cm, 4 cm) in one model and (1.5 cm , 6 cm) in a second model. The Debye parameters for skin obtained from published data by Gabriel *et al.* [22], while the Debye parameters for malignant tissue are those used by Bond [6]. The Debye parameters for each type of tissue are shown in Table I.

The grid resolution, dx, is 0.5mm and the time step dt is defined as 0.833ps ($dt = \frac{dx}{2c}$). Each data-independent imaging technique is applied to an identical breast imaging scenario and artifact removal system. As a preprocessing step, an ideal artifact removal algorithm, described previously by Bond *et al.* [6] was used to remove the early stage artifact and reflections from the air skin interface. Before further processing, the signals are downsampled from 1200 GHz (the time step in the FDTD simulation) to 50 GHz. The input signal is a 150-ps differentiated Gaussian pulse, with a center frequency of 7.5 GHz and a -3db bandwidth of 9 GHz.

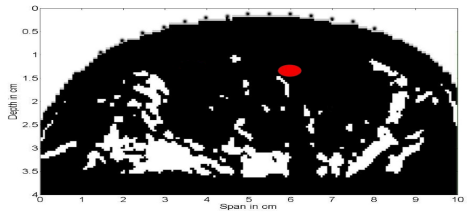

Fig. 4. Antenna configuration of breast model with a malignant lesion located at a depth of 1.5 cm and span of 6 cm

A malignant tumor is modeled at (1.5 cm, 6 cm) in Figures 1, 2 and 3, indicated by a pink circle. Resultant lesion scatterers are located 1 to 3 mm shallower than the modeled tumor location, as its response is assumed as a point scatterer. System performance is evaluated in terms of the Signal to Clutter ratio (S/C), which is defined as the ratio of maximum energy at the tumor location to the energy at the same location in a tumor-free model, as in [6]. The S/C results are documented in Table II for the inclusion of a single tumor located at (1.5 cm, 6 cm) and at (1.5 cm, 4 cm) (though lack of space precludes inclusion of images for these cases). In all images, backscattered energy from regions of fibroglandular tissue within the breast are clearly visible. For each algorithm, the multistatic approach offers superior clutter suppression compared to the corresponding monostatic algorithms. Figure 1 illustrates a monostatic and multistatic DAS beamformed image respectively. The Multistatic MIST (Figure 3(b)) configuration [16] offers an improved S/C ratio over DAS (Figure 1(b)), allowing an examination of the fibroglandular distribution within the breast. However, Lim's improved DMAS system [15], shown in Figure 2 has the best S/C ratios for both monostatic and multistatic antenna configurations, for this particular test scenario.

VIII. Conclusion

In this paper, a representative selection of existing data-independent UWB breast imaging algorithms have been described. Results indicate that DMAS outperforms both the DAS and MIST for the relatively simple testing scenario examined here. The assumption of an ideal artefact removal algorithm may be responsible for the significant S/C differences between the monostatic and multistatic results of each beamforming method.

The MIST beamformer is designed to compensate for propagation effects within the breast, therefore it is likely to outperform DMAS when lesions are located closer to the chest wall. DMAS and DAS do not accommodate for any attenuation and phase effects. An optimal data-independent beamforming solution which incorporates elements of both DMAS and MIST is currently in development. Future work will involve testing the algorithms in an even more difficult imaging scenario where the tumor is surrounded by fibroglandular tissue in very dense breast tissue.

References

[1] A. C. Society, "Cancer facts and figures 2008," *American Cancer Society*, 2008.

[2] S. L. Nass, I. C. Henderson, and J. C. Lashof, *Mammography and Beyond: Developing Technologies for the early detection of breast cancer*. National Academy Press, 2001.

[3] S. C. Hagness, A. Taflove, and J. E. Bridges, "Two-dimensional FDTD analysis of a pulsed microwave confocal system for breast cancer detection: Fixed focus and antenna array sensors," *IEEE Trans. Biomed. Eng.*, vol. 45, pp. 1470–1479, 1998.

[4] ——, "Three-dimensional FDTD analysis of a pulsed microwave confocal system for breast cancer detection: Design of an antenna array element," *IEEE Trans. Antennas and Propagat.*, vol. 47, pp. 783–791, May, 1999.

[5] E. C. Fear, X. Li, S. C. Hagness, and M. A. Stuchly, "Confocal microwave imaging for breast cancer detection: Localization of tumors in three dimensions," *IEEE Trans. Biomed. Eng.*, vol. 47, pp. 812–812, 2002.

[6] E. J. Bond, X. Li, S. C. Hagness, and B. D. V. Veen, "Microwave imaging via space-time beamforming for early detection of breast cancer," *IEEE Trans. Antennas and Propagat.*, pp. 1690–1705, 2003.

[7] S. K. Davis, E. J. Bond, X. Li, S. C. Hagness, and B. D. V. Veen, "Microwave imaging via space-time beamforming for the early detection of breast cancer: Beamformer design in the frequency domain," *J. Electromagnet. Wave.*, vol. 17, pp. 357–381, 2003.

[8] Y. Xie, B. Guo, L. Xu, J. Li, and P. Stoica, "MultiStatic Adaptive Microwave Imaging for Early Breast Cancer Detection," *IEEE Trans. Biomed. Eng.*, vol. 53, no. 8, pp. 1647–1657, 2006.

[9] S. S. Chaudhary, R. K. Mishra, A. Swarup, and J. M. Thomas, "Dielectric properties of normal and malignant human breast tissue at radiowave and microwave frequencies," *Indian J. Biochem. Biophys.*, vol. 21, pp. 76–79, 1994.

[10] W. Joines, Y. Zhang, C. Li, and R. L. Jirtle, "The measured electrical properties of normal and malignant human tissues from 50 to 900 MHz," *Med. Phys*, vol. 21, pp. 547–550, 1993.

[11] J. Jossinet, "The impedivity of freshly excised human breast tissue," *Physiol. Meas.*, vol. 19, pp. 61–75, 1998.

[12] B. D. V. Veen and K. M. Buckley, "Beamforming: A versatile approach to spatial filtering," *IEEE ASSP Magazine*, April 1988.

[13] X. Li and S. C. Hagness, "A confocal microwave imaging algorithm for breast cancer detection," *IEEE Microwave and Wireless Components Letters*, vol. 11, pp. 130–132, 2001.

[14] R. Nilavalan, S. C. Hagness, and B. D. V. Veen, "Numerical investigation of breast tumour detection using multi-static radar," *IEE Electronic Letters*, vol. 39, no. 25, pp. 1787–1789, Dec. 2003.

[15] H. B. Lim, N. T. T. Nhung, E.-P. Li, and N. D. Thang, "Confocal microwave imaging for breast cancer detection: Delay-multiply-and sum image reconstruction algorithm," *IEEE Transactions on Biomedical Engineering*, vol. 55, no. 6, pp. 1697–1704, June 2008.

[16] M. O'Halloran, M. Glavin, and E. Jones, "Quasi-Multistatic MIST Beamforming for the Early Detection of Breast Cancer," *IEEE Trans. Biomed. Eng., In Press*.

[17] A. Taflove and S. C. Hagness, *Computational Electrodynamics: The Finite-Difference Time-Domain Method*. Artech House Publishers, June, 2005.

[18] D. M. Sullivan, *Electromagnetic simulation using the FDTD method*. IEEE Press Series on RF and Microwave Technology, 2000.

[19] R. Leubbers, F. Hunsberger, K. Kunz, R. Strandler, and M. Schneider, "A frequency-dependent finite-difference time-domain formulation for dispersive materials," *IEEE Trans. Electromag. Compat.*, vol. EMC-32, pp. 222–227, Aug. 1990.

[20] M. Lazebnik, L. McCartney, D. Popovic, C. B. Watkins, M. J. Lindstrom, J. Harter, S. Sewall, A. Magliocco, J. H. Booske, M. Okoniewski, and S. C. Hagness, "A large-scale study of the ultrawideband microwave dielectric properties of normal breast tissue obtained from reduction surgeries," *Phys. Med. Biol.*, vol. 52, pp. 2637–2656, 2007.

[21] M. Lazebnik, D. Popovic, L. McCartney, C. B. Watkins, M. J. Lindstrom, J. Harter, S. Sewall, T. Ogilvie, A. Magliocco, T. M. Breslin, W. Temple, D. Mew, J. H. Booske, M. Okoniewski, and S. C. Hagness, "A large-scale study of the ultrawideband microwave dielectric properties of normal, benign and malignant breast tissues obtained from cancer surgeries," *Phys. Med. Biol.*, vol. 52, pp. 6093–6115, 2007.

[22] C. Gabriel, S. Gabriel, and E. Corthout, "The dielectric properties of biological tissues: I. Literature survey," *Phys. Med. Biol.*, vol. 41, pp. 2231–2249, 1996.